JOURNAL OF MATERIALS SCIENCE 11 (1976) 2068–2074

Further observations on the plastic deformation of a normalized low carbon steel

R. G. LUTHER
Mechanical Engineering Department, Salisbury College of Technology, Salisbury, UK
T. R. G. WILLIAMS
Mechanical Engineering Department, University of Southampton, Southampton, UK

The plastic deformation of a commercial grade low carbon steel has been investigated using microhardness and grain strain measurement techniques. Two distinct modes of deformation during plastic flow in low carbon ferritic steel have been identified. The initial stage involves the propagation of the Luder's band along the gauge length of the sample by slip strain in the surface and near surface grains only, the strain accommodation in the interior of the material being attained by a predominantly grain translation mode. The second stage involves the propagation of a strain hardening front through the cross-section of the material as the macro-strain is increased through the flow stress region.

1. Introduction

In a recent paper, the authors [1] presented evidence of heterogeneous macro-plastic deformation occurring throughout the cross-section of a tensile test piece during yielding and flow strain. The term macro-plastic deformation is used to differentiate between the plastic flow noted in these observations and the localized heterogeneous deformation within individual grains envisaged by Ashby [2] and demonstrated by Boas and Hargreaves [3] using hardness surveys. Luther and Williams [1] also used hardness surveys to trace the strain-hardening contours and a wave pattern was revealed involving plastic yielding, originating at the free surface, and propagating through the cross-section during progressive straining through the flow stress range, to attain uniform strain hardening at plastic instability. Reinforcing the relatively weak surface grains prevented the heterogeneous plastic deformation between the surface and the core of the material and increased the yield stress. With progressively deeper reinforcement layers, the yield strength of the material was raised to the nominal stress at which plastic instability was attained in the unreinforced steel, but at this reinforcement depth the yield strength reached a maximum. The present paper presents an extension of this work, using both hardness and grain strain measurement techniques to investigate the heterogeneous macro-plastic behaviour within the flow stress region of the stress–strain diagram of the unreinforced samples. Further work on reinforced samples will be presented in a subsequent paper.

2. Experimental technique

The material composition, heat-treatment and static mechanical properties were as stated previously [1]. A statistical analysis of the grains showed the structure to be equi-axed with a grain size of $17.5 \pm 0.3\,\mu m$ for 95% confidence. For all of the tests, the gauge length of the specimens was electropolished to eliminate any damage caused by the manufacturing process. Tensile straining was carried out in an Instron machine at a strain-rate of $0.05\,min^{-1}$. To reduce clamping and misalignment effects, the 4 mm diameter specimens were loaded through spherical end seatings in addition to the standard universal joint couplings.

Macro-strain measurements were determined both from changes in area and gauge length. For the former, the sample diameter was measured before and after straining by means of an optical projector, and for the latter, the change in length was derived using a travelling microscope. In each case the apparatus was calibrated by means of calibrated slip gauges so that dimensions could be determined to within 10^{-3} mm. For the purpose of this work, the strain derived from the expression $\ln (A_0/A)$ has been designated ϵ_A whilst that derived from $\ln (l/l_0)$, within the uniform plastic flow region, has been designated ϵ_l. General macro-strain has been indicated by ϵ.

During creep deformation two modes of plastic deformation are possible, slip strain and grain-boundary sliding. Several methods exist which enable the relative contribution of slip strain and grain-boundary sliding to be assessed in relation to the total strain; these include internal and external markers [4, 5] and changes in the grain shape [6]. The latter technique is simple to use and requires no special specimen preparation for internal measurements. However, it has been justifiably criticised [5, 7] on account of the fact that grain shape measurements may over-estimate the degree of grain-boundary sliding since migration may result in the elongated grains returning to their original equi-axed condition. Similarly, it has been suggested [8] that the grain shape at as-cut surfaces may change during creep tests, thus giving anomalous grain-boundary sliding results. These criticisms, however, do not apply at room temperature, and this technique has therefore been used throughout the work. It can be shown that the true grain strain (ϵ_G) can be represented by the expression $\epsilon_G = \ln (L/B)^{2/3}$ where L is the mean length of the grains and B the mean width, using the loading axis as the reference direction.

Both the hardness and the dimensions for L and B were determined from as-cut surfaces taken from specimens strained to pre-determined values within the flow stress range. The hardness surveys were conducted on a cord line passing through the centre of the specimen, using a dead weight machine and a 50 g load giving Vickers Diamond Pyramid values. The individual values for L and B were the maximum dimensions of each grain measured when taken from sections parallel to the straining axis, the total number of grains measured at each macro-strain level was > 300. In all cases, the as-cut surfaces were electropolished to remove all traces of damage induced by the preparation process. Measurements of L and B were taken from two regions of the specimen cross-section, one from the centre and one from a point equal to $0.9R$ where R was the radius of the sample.

3. Experimental results

The hardness surveys presented in Fig. 1 indicate that plastic deformation of the specimen is initiated

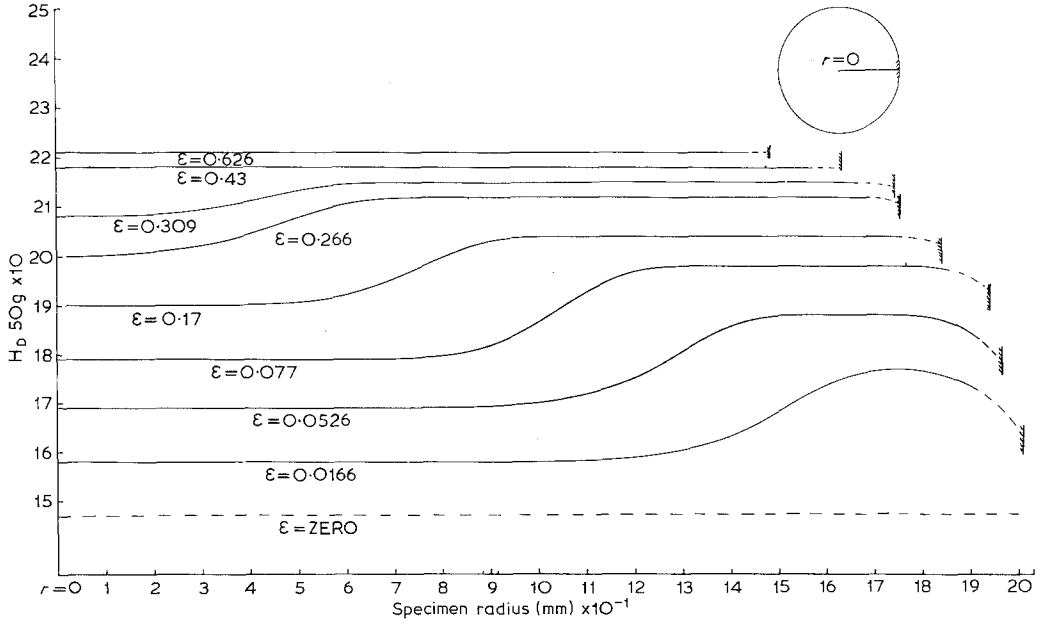

Figure 1 Micro-hardness survey of tensile specimens strained to particular values.

TABLE I Tabulated data for ϵ_A and related true grain strain (ϵ_G)

ϵ_A	Grain strain			
	Centre	95% confidence limits ±	At $r = 0.9R$	95% confidence limits ±
0.0166	0.007 62	0.02	0.059 52	0.02
0.0526	0.036 00	0.02	0.119 42	0.02
0.1700	0.163 96	0.02	0.226 34	0.02
0.3090	0.324 30	0.028	0.345 66	0.028
0.4300	0.413 60	0.03	0.440 83	0.03
0.6200	0.678 03	0.03	0.582 22	0.03

at the surface and progresses through the section of the sample as the strain increases. At the end of the Luder's strain, $\epsilon_A = 0.0166$, the highest hardness occurs at about 0.25 mm below the surface, the hardness value at this point being about 20 units greater than that at the centre of the test pieces. As the macro-strain is increased there is a progressive strain hardening over the whole cross-section, but the degree of strain hardening is more advanced at the surface, and the boundary of the differential strain hardening traverses the cross-section as a wave. Between $\epsilon_A = 0.3$ and 0.4, the wave reaches the centre of the sample giving uniform hardness values over the whole cross-section and this hardness plateau then increases with strain until fracture supervenes.

Table I lists the grain strain estimated for various macro strain values both at the centre of the test pieces and at a radius equal to $0.9R$. The relative contributions of slip strain and grain translation movement can be derived using the ratio of grain strain (ϵ_G) to macro-strain (ϵ). Where deformation is caused by slip strain only then $\epsilon_G/\epsilon \geqslant 1$, and if no change in grain shape occurs then $\epsilon_G/\epsilon = 0$. Grain strain results, tabulated in this form, are given in Table II, and shown diagrammatically in Fig. 2. For the centre of the specimen, these results reveal predominantly grain translation deformation for samples strained to the end of the Luder's plateau, slip strain accounting for only about 40% of the total deformation. At about 5% macro-strain, $\epsilon_G/\epsilon = 0.8$ and this ratio becomes unity in the macro strain range 10 to 15%. In contrast, the near surface grain strain is initially four times that of the macro-strain and does not reduce to unity until $\epsilon_A \simeq 0.25$.

TABLE II Tabulated data relating ϵ_G and ϵ_G/ϵ_A ratio

ϵ_A	True grain strain, ϵ_G			
	Centre		$r = 0.9R$	
	ϵ_{GC}	ϵ_{GC}/ϵ_A	ϵ_{GS}	ϵ_{GS}/ϵ_A
0.0166	0.007 62	0.4590	0.59 52	3.585 54
0.0526	0.036 00	0.6844	0.119 42	2.270 34
0.1700	0.163 96	0.9644	0.226 34	1.331 41
0.3090	0.324 30	1.0495	0.345 66	1.118 64
0.4300	0.413 60	0.9613	0.440 83	1.025 18
0.6200	0.678 03	1.0935	0.582 22	0.939 06

Fig. 3 shows both the relationship between the macro-strain values, determined assuming that constant volume conditions apply within the flow stress region, and the corresponding points derived experimentally from strain measurements. Within the apparent uniform plastic deformation range, that is up to $\epsilon = 'n'$, the assumption that $A_0 l_0 = Al$ would predict a linear relationship between ϵ_A and ϵ_l, but this appears to be true only over the strain range between $\epsilon = 0.1$ and 0.2, and below $\epsilon = 0.1$ the strains determined from axial measurements are the larger. It thus appears that constant volume conditions do not obtain until strains in

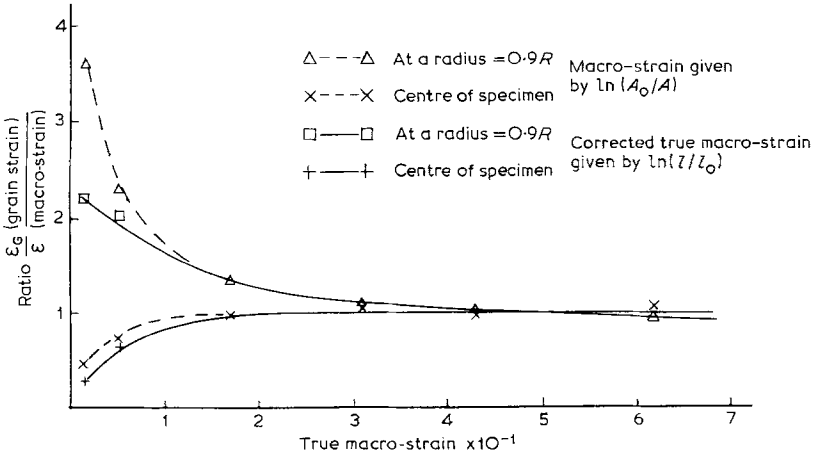

Figure 2 Relationship between the ratio of true grain strain (ϵ_G)/true macro-strain (ϵ) and true macro-strain (ϵ).

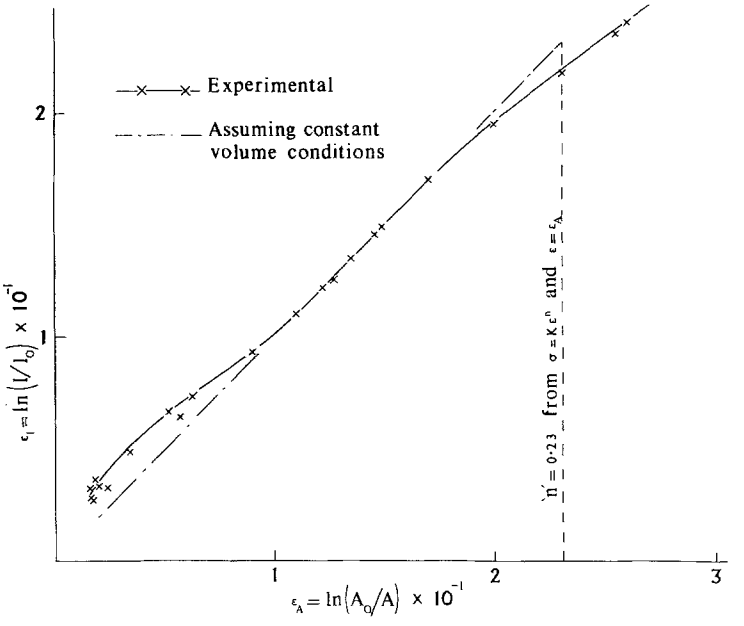

Figure 3 Relationship between macro strains ϵ_A and ϵ_l.

excess of the Luder's strain are reached. Another feature of the results shown in Fig. 3 is the apparent strain at which instability occurs. An analysis of the true stress–strain data using $\sigma = K\epsilon^n$, where ϵ is given by $\ln(A_0/A)$, gave a value of $n = \epsilon = 0.23$ whereas the value obtained from Fig. 3 is about 0.19. Thus the expressions $\ln(L/B)^{2/3}$ and $\ln(A_0/A)$ do not accurately describe the amount of strain below $\epsilon = 0.1$ as they both assume that constant volume conditions apply and that Poisson's ratio = 0.5. It is therefore necessary to correct the values of strain within this region and an expression for the axial grain strain incorporating an experimentally derived value for Poisson's ratio is given by $\epsilon_G = \ln[1 + (L - B)/(B + \nu L)]$ whilst for the macro strain value the most appropriate value appears to be given by $\ln(l/l_0)$. Using these two expressions for strains < 0.1 the corrected values of ϵ_G/ϵ given in Table III were obtained and, these values are also included in Fig. 2. At the end of the Luder's strain the near surface grain strain is now about twice that of the macro strain, whilst the deformation in the centre of the sample involves about 30% slip strain and 70% grain translation movement.

Fig. 4 shows the initial portion of typical load–extension diagrams for a series of samples given various surface treatments. Curve (a) was typical of an electropolished sample strained only sufficiently to produce the yield drop. Curve (b) was subsequently produced from sample (a) which had been machined to reduce the gauge length diameter by just over 1 mm, and electropolished and re-strained. Both the yield drop and Luder's strain are still present in the sample. Curve (c) was typical of electropolished samples strained to the end of the Luder's strain, whilst curve (d) resulted from restraining of sample (c) following remachining and electropolishing of the gauge length to reduce its diameter by approximately

TABLE III Tabulated data relating ϵ_A and corrected true grain strain/corrected true strain ratio

ϵ_A	True grain strain, ϵ_G				Experimentally derived values for Poisson's ratio at $\epsilon = \epsilon_A$
	Centre		$r = 0.9R$		
	ϵ_{GC}	ϵ_{GC}/ϵ	ϵ_{GS}	ϵ_{GS}/ϵ	
0.0166	0.009 10	0.2843	0.070 00	2.1875	0.3
0.5626	0.040 00	0.6153	0.131 00	2.0100	0.42
0.1700	0.163 96	0.9644	0.226 34	1.3314	0.5
0.3090	0.324 30	1.0495	0.345 66	1.1186	0.5
0.4300	0.413 60	0.9613	0.440 83	1.0252	0.5
0.6200	0.678 03	1.0935	0.582 22	0.9391	0.5

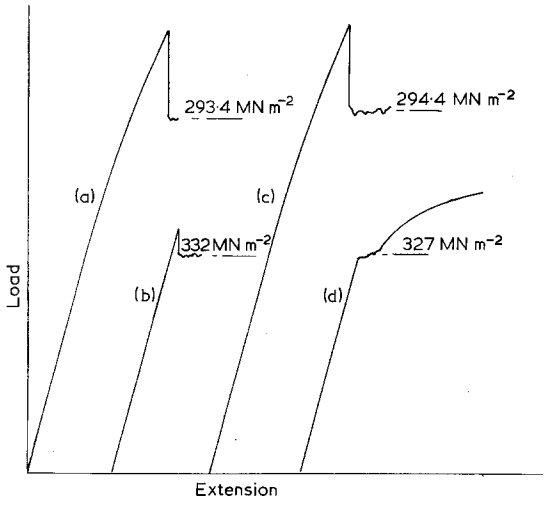

Figure 4 Typical partial load–extension diagrams for: (a) electropolished sample strained to the beginning of the Luder's strain; (b) speciman (a) subsequently re-machined along the gauge length reducing the diameter by about 27%, electropolished and re-strained to the end of the Luder's strain; (c) electropolished sample strained to the end of the Luder's strain; (d) specimen (c) treated as in (b) and re-strained beyond the Luder's strain.

1 mm. Although the yield drop is removed, the Luder's strain remains, but it appears to propagate on a rising stress. Furthermore, the lower yield stress was of a higher stress value than that obtained for the electropolished samples strained only once.

4. Discussion of results

The hardness surveys presented in Fig. 1 indicate that strain hardening, and therefore plastic deformation, can occur in a heterogeneous manner during tensile straining and that plastic deformation at yielding originates at the weakly constrained surface grains. This plastic behaviour may be described in two distinct stages. At the end of the Luder's strain there is a general increase in hardness of some 10 Vickers Pyramid units in the centre of the specimen, but the surface layers have increased by about 30 units. This differential hardening appears to be associated with a plastic wave superimposed over the general deformation pattern. Since the Luder's strain simply represents the passage of plastic deformation along the gauge length of the sample, the implication is that the differential deformation is initiated at the upper yield point and occurs during the yield drop. As the strain is increased beyond the Luder's plateau there is a progressive strain hardening over the whole cross-section, but the degree of strain hardening is more advanced near the surface and with increasing strain this additional plastic deformation traverses the cross-section as a plastic wave. Between $\epsilon = 0.3$ and 0.4, the wave reaches the centre of the sample giving uniform hardness values over the whole cross-section. This hardness plateau increases with strain until fracture supervenes.

The grain strain measurements given in Fig. 2 also reveal that plastic deformation over the cross-section is hetergeneous, the degree of heterogeneity decreasing as the macro-strain is increased, being eliminated at about 30% strain. In addition, these results suggest that, in the early stages of plastic deformation, the mode of deformation in the centre of the material is not the same as that operating near the surface. At the centre the deformation consists of about 30% slip strain whilst the remainder appears to be a form of grain translation or grain-boundary sliding. Near the surface, and presumably at the surface, the deformation appears to be pure slip strain, the magnitude of which is about twice that of the macro value. This does not mean that the total elongation is any greater than the macro value, but simply that the near surface grains experience a greater strain than that indicated by the macro measurements. Evidence in support of such differential plastic deformation is obtained in the work on Tandon and Tangri [9]. These authors used 3% silicon iron to investigate the early stages of tensile deformation. Etch-pit studies of samples strained up to the macro yield point revealed premature plastic deformation in the surface layers, and for samples strained to approximately the end of the Luder's plateau, whilst 100% of the surface grains revealed evidence of slip only 40% of the grains in the centre of the material showed slip activity. Further evidence of the apparent "elastic" behaviour of the constrained interior grain structure during the initial stages of plastic flow is given in Fig. 4. For the sample strained to the yield drop and subsequently machined and electropolished to reduce its diameter, a yield drop is again observed when the material is re-strained. The yield drop, however, is absent in similar samples previously strained to the end of the Luder's plateau, but the Luder's strain is still visible albeit on a rising stress. Also the Luder's strain, during the second tests, occurs at a stress level about 30 MN m^{-2} higher than during the initial straining.

Grain translation or grain-boundary sliding is usually associated with creep behaviour at high temperatures and low strain-rates, and has been investigated for a variety of metals. Nevertheless, the phenomenon has been reported to occur at room temperature in magnesium and its alloys and aluminium and its alloys [10–12]. Also, the proportion of the total deformation contributed by grain-boundary sliding increases with decrease in grain size [13, 14]. In general, the model presented to account for grain translation involves the migration of grain boundaries to accommodate the strain and to enable an equi-axed structure to be retained. However, grain-boundary sliding is associated with strain-rates in the order of $2 \times 10^{-5} \text{min}^{-1}$ and does not appear to have been reported for the strain-rates used in this work, that is $5 \times 10^{-2} \text{min}^{-1}$. It is also difficult to envisage that a model involving diffusion can have sufficient time to operate at room temperature, unless internal heating of the material occurs. Possibly, therefore, the grain translation which occurs at low strains in this work results from localized shearing at the grain boundary. If a porportion of these grains deform considerably more than neighbouring ones, because of favourable orientation, on the one hand, and constraint, on the other, the strain has to be accommodated either by void formation between the grains or by movement of the adjacent grains. Such movement may possibly be affected by localized shearing of the high spots, followed by ratcheting or rotational movement of the grains less favourably oriented for slip. However, Langdon [5] has suggested a model for the apparent grain-boundary sliding (Langdon's definition: low temperature shear) observed during creep at room temperature. He suggests that at a boundary between two grains, one of which is oriented more favourably for slip, conditions of strain continuity will give rise to a localized zone of accommodating deformation near the grain boundary in one or the other of the grains. This results in a round "off" at the edge of the less favourably oriented grain or the inhibition of slip in the favourably oriented one. At present, however, there is insufficient information available to make definitive statements on the exact mechanism involved. Nevertheless, the evidence presented here suggests that two concurrent modes of plastic deformation are present at low strains during tensile straining and for the second one to occur, it has to be triggered off by slip strain in the weakly constrained surface grains. In conclusion, a current theory for yielding in fine grained iron, relates the upper yield point with the stress at which slip first penetrates a grain boundary, both at the surface and interior of the material. The Luder's plateau then represents the stress at which the Luder's band propagates along the gauge length by slip strain throughout the cross-section of the sample. Since the mode of deformation in the interior of the material is predominantly of a grain-boundary mode, the Luder's band propagation appears to be confined to the surface and near surface grains of the material.

5. Conclusions

Two distinct modes of deformation during plastic flow in low carbon ferritic steel have been identified. The initial stage involves the propagation of the Luder's band along the gauge length of the sample by slip strain in the surface and near surface grains only, the strain accommodation in the interior of the material being attained by a predominantly grain translation mode. The second stage involves the propagation of a strain hardening front through the cross-section of the material as the macro-strain is increased through the flow stress region.

Acknowledgements

The authors would like to express their gratitude to Professor R. L. Bell, of the University of Southampton, and the Principal of the Salisbury College of Technology, for providing facilities for this work, and to Miss D. G. Mitchell, who typed the manuscript.

References

1. R. G. LUTHER and T. R. G. WILLIAMS, *J. Mater. Sci.* 9 (1974) 136.
2. M. F. ASHBY, *Phil. Mag.* 21 (1970) 399.
3. W. BOAS and M. E. HARGREAVES, *Proc. Roy. Soc.* A193 (1948) 89.
4. C. GRAEME-BARKER, Ph.D. Thesis, University of London (1967).
5. T. G. LANGDON, D.I.C. Thesis, University of London (1965).
6. W. A. RACHINGER, *J. Inst. Metals* 81 (1952–53) 33.
7. R. L. BELL, C. GRAEME-BARKER and T. G. LANGDON, *Trans. Met. Soc. AIME* 239 (1967) 1821.
8. R. C. GIFKINS, *Bull. Inst. Met.* 3 (1957) 185.
9. K. N. TANDON and K. TANGRI, *Met. Trans. A.* 6A (1975) 809.

10. R. C. GIFKINS and T. G. LANGDON, *J. Inst. Metals* **93** (1964–65) 347.
11. A. B. CHANDURI, J. E. MAHAFFY and N. J. GRANT, *Acta. Met.* **7** (1959) 60.
12. F. B. CUFF and N. J. GRANT, *Trans. AIME* **212** (1958) 355.
13. D. MCLEAN, *J. Inst. Metals* **81** (1952) 293.
14. R. C. GIFKINS, *J. Aust. I.M.* 8 (1963) 148.

Received 23 January and accepted 30 April 1976.